

# Chemical Science



**Accepted Manuscript** 

This article can be cited before page numbers have been issued, to do this please use: D. Chatzogiannakis, V. Arszelewska, P. Cabelguen, M. R. Palacín and M. Casas-Cabanas, *Chem. Sci.*, 2025, DOI: 10.1039/D5SC06660C.



This is an Accepted Manuscript, which has been through the Royal Society of Chemistry peer review process and has been accepted for publication.

Accepted Manuscripts are published online shortly after acceptance, before technical editing, formatting and proof reading. Using this free service, authors can make their results available to the community, in citable form, before we publish the edited article. We will replace this Accepted Manuscript with the edited and formatted Advance Article as soon as it is available.

You can find more information about Accepted Manuscripts in the <u>Information for Authors</u>.

Please note that technical editing may introduce minor changes to the text and/or graphics, which may alter content. The journal's standard <u>Terms & Conditions</u> and the <u>Ethical guidelines</u> still apply. In no event shall the Royal Society of Chemistry be held responsible for any errors or omissions in this Accepted Manuscript or any consequences arising from the use of any information it contains.



This article is licensed under a Creative Commons Attribution-NonCommercial 3.0 Unported Licence Open Access Article. Published on 17 2025. Downloaded on 2025/11/18 11:53:26.

View Article Online DOI: 10.1039/D5SC06660C

# **ARTICLE**

# Addressing first cycle irreversible capacity in lithium-rich layered oxides by blending with delithiated active materials

Received 00th January 20xx. Accepted 00th January 20xx

DOI: 10.1039/x0xx00000x

Dimitrios Chatzogiannakis<sup>a,b,c</sup>, Violetta Arszelewska<sup>d</sup>, Pierre-Etienne Cabelguen<sup>d</sup>, M. Rosa Palacin<sup>a\*</sup>, Montse Casas-Cabanasb,e,\*

Lithium-rich oxides (LRO), derived from NMC-type materials, are among the most promising next-generation positive electrode candidates for lithium-ion batteries. Despite their potential, their practical application is hinderend byinherently low first-cycle coulombic efficency, caused by the irreversible loss of lithium during the initial cycle. In this work, we address this drawback by chemically delithiating secondary active materials -LiMn<sub>2</sub>O<sub>4</sub> (LMO) or LiFePO<sub>4</sub>- and subsequentyly blending them with the cobalt-free lithium rich oxide Li<sub>1/15</sub>Ni<sub>0/3</sub>Mn<sub>0/55</sub>O<sub>2</sub>. The incorporation of these delithiated components improves first-cycle efficiency, with the degree of enhancement proportional to the fraction of added material, and capacity retention, while only modestly reducing overall capacity. Differential scanning calorimetry (DSC) further reveals improved thermal stability for LRO:FePO<sub>4</sub> blends evidenced by a higher decomposition temperature and lower overall heat released. In contrast, LRO:λ-MnO<sub>2</sub> blends show increased moisture sensitivity. Operando synchrotron X-ray diffraction confirms that the secondary active material actively participates in the electrochemical processes of the blends. Our findings demonstrate a simple, industry-compatible strategy to mitigate one of the major drawbacks of LROs, paving the way for more sustainable and high performance lithium-ion batteries.

# Introduction

As efforts towards sustainable transportation intensify, Electric Vehicles (EVs) are becoming increasingly popular. However, the batteries powering them (predominantly Li-ion systems) still require significant improvement. These batteries were originally developed for portable electronics, which have different performance requirements. As a result, key challenges remain in meeting the requisites of EVs, and include the need for higher power output, enhanced safety, and improved longevity under sustained highperformance use.

One of the critical components of a Li-ion battery is the positive electrode, with layered oxides among the most commonly used materials. These have a general formula LiMO<sub>2</sub> where M = Co, Mn, Ni, Al or their combinations. The most representative families of

The most commonly used blends contain layered oxides. For instance, when LMO is mixed with NMC it has been observed that, even though the total specific capacity of the electrode decreases, the overall lithium exchange kinetics of the electrode improve. Moreover, such blended electrode can exhibit additional performance gains due to the synergistic interaction between components, including higher energy density than predicted from the rule of mixture, especially at high rates, and also lower capacity fading, the latter being attributed to suppressed manganese dissolution (6,7). During cycling, the effective rate experienced by a material within a blend can differ significantly from the nominal cell

Supplementary Information available: [details of any supplementary information available should be included here]. See DOI: 10.1039/x0xx00000x

layered oxides are LiNi<sub>x</sub>Mn<sub>y</sub>Co<sub>z</sub>O<sub>2</sub> where x+y+z=1, commonly referred to as NMCs, and LiNi<sub>x</sub>Co<sub>v</sub>Al<sub>z</sub>O<sub>2</sub> where x+y+z=1, known as NCAs. Other materials commonly present in commercial batteries are LiFePO<sub>4</sub> (LFP), with olivine structure, and the spinel LiMn<sub>2</sub>O<sub>4</sub> (LMO). Each of these materials offers distinct advantages and drawbacks. In general, layered oxides provide the highest reversible capacities, LFP is recognized for its longest cycle life, safety and costeffectiveness, and LMO features very fast lithium kinetics while maintaining low cost, though it generally suffers from lower capacity and shorter cycle life compared to other options (1,2). To tailor electrode performance to the application needs, blended electrodes combining multiple active materials are often utilized in EV batteries. Yet, its composition is usually decided based on empirical criteria, with few studies attempting to rationalize the interactions between different active materials (3-5).

<sup>&</sup>lt;sup>a</sup> Institut de Ciència de Materials de Barcelona, ICMAB-CSIC, Campus UAB, 08193

Centro de Investigación Cooperativa de Energías Alternativas (CIC energiGUNE), Basque Research and Technology Alliance (BRTA), 01510 Vitoria-Gasteiz, Spain

<sup>&</sup>lt;sup>c</sup> ALISTORE-ERI, CNRS FR, 3104, France

<sup>&</sup>lt;sup>d</sup> UMICORE, 31 rue du Marais, 1000, Brussels, Belgium

<sup>&</sup>lt;sup>e</sup> Ikerbasque - Basque Foundation for Science, Maria Diaz de Haro 3, 48013 Bilbao, Spain

hemical Science Accepted Manusc

**Journal Name** 

rate and blend components can bear more or less current depending on the state of charge of the cell and the intrinsic reaction kinetics of the active materials (8).

On the other hand, safety concerns related to EVs mainly revolve around their battery related hazards. Malfunction, operation out of specifications and physical abuse of the battery can result in the increase of its temperature, either by heat released from the cell itself or an external heat source (e.g. malfunctioning nearby battery cell) Catastrophic failure typically occurs when the battery exceeds a critical temperature threshold (9) (10), causing a phenomenon known as thermal runaway. During such an event, large amounts of heat are released, triggering a series of exothermic processes that can result in fire, or explosion. The positive electrode plays a crucial role in this phenomenon as its thermal stability and interaction with other components can significantly influence the risk of thermal runaway (11,12). Additionally, many of the active materials release oxygen when heated, which can fuel combustion in the presence of the flammable organic compounds used as electrolyte solvents in Liion batteries (13). Studies on active materials have been carried out to increase this critical runaway temperature and/or reduce the heat released during the event through chemical substitutions, coatings or electrolyte modification (14,15). Blending different active materials has also been explored to improve safety in Li-ion batteries (16).

A very promising family of next-generation positive active materials meant for EVs is the so called lithium-rich layered oxides (LROs) (13,17). Their chemical formula and crystal structure derive from that of layered oxides, yet have a Li/M ratio higher than 1 and can therefore be described as  $Li_{1+x}M_{1-x}O_2$  where typically  $0 < x \le 0.33$ (18). These materials offer very large reversible specific capacities able to exceed 250 mAh/g, due to the participation of lattice oxygen in the redox reaction during cycling (19-21). However, structural changes often involving oxygen release result in significant first-cycle irreversibility, manifesting as low initial coulombic efficiencies (typically around 80%) and poor retention over time. This irreversibility is closely linked to a voltage plateau above 4.5 V during the first battery charge, commonly referred to as "activation", during which a large amount of lithium is extracted that cannot be completely reaccommodated in the crystal structure upon the subsequent discharge. Thus, there is a fraction of lithium that remains inactive at the negative electrode, which has a detrimental effect to the cell energy density (22). Additionally, thermal stability is also a major concern, as oxygen loss and structural instability, among other factors, also contribute to a lower onset temperature for thermal decomposition (23,24).

A limited number of studies have suggested mitigating this loss by incorporating lithium-accepting compounds into positive electrode that can reversibly host lithium ions during cycling. This can be done either by physical blending or as a surface coating. In the seminal work by Lee and Manthiram (25,26) LRO Li[Li $_{0.2}$ Mn $_{0.54}$ Ni $_{0.13}$ Co $_{0.13}$ ]O2 was combined with V $_2$ O5, Li $_4$ Mn $_5$ O $_{12}$  or LiV $_3$ O $_8$  which act as lithium

acceptors. These additions enabled reinsertion of lithium rinto the acceptor after the first charge, thereby reducing the acceptor after the need for excess graphite. Another similar strategy developed later has been the modification of an LRO to form surface and bulk domains of  $\lambda$ -MnO<sub>2</sub> (the delithiated form of LMO) (27–29) or coating with amorphous FePO<sub>4</sub>. Both strategies were shown to improve the first cycle coulombic efficiency for the positive electrode.

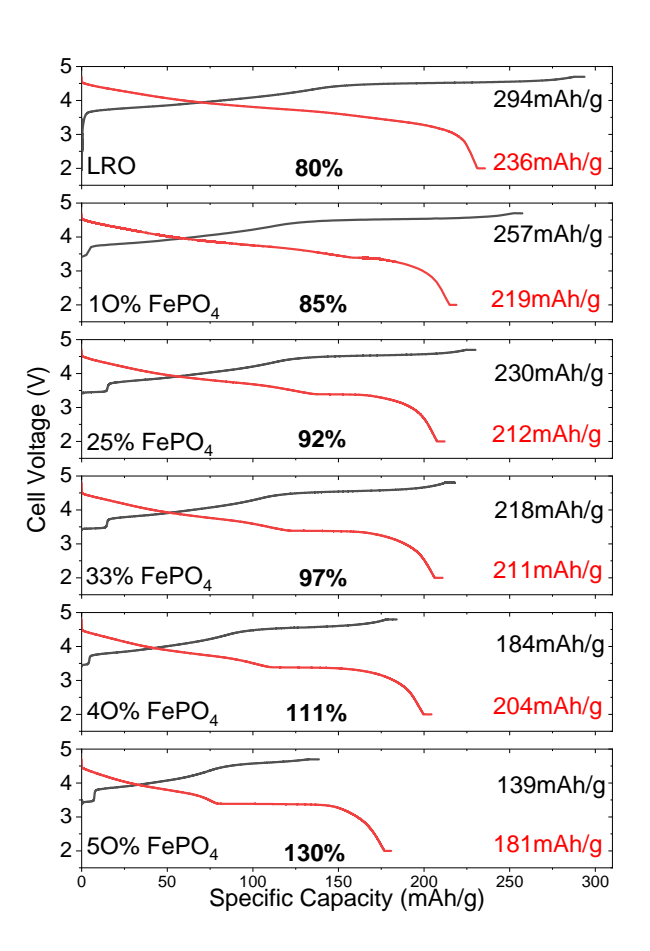
In the present work, we introduce a simplified approach that involves blending LRO with a chemically delithiated commercial positive electrode material to act as lithium acceptor, in this case FePO<sub>4</sub> or  $\lambda$ -Mn<sub>2</sub>O<sub>4</sub>. The composition Li<sub>1.15</sub>Ni<sub>0.3</sub>Mn<sub>0.55</sub>O<sub>2</sub> was selected (formally within the solid solution between Li<sub>2</sub>MnO<sub>3</sub> and LiNi<sub>0.5</sub>Mn<sub>0.5</sub>O<sub>2</sub>) as it does not contain any cobalt (toxic and expensive) and delivers high energy density (30,31). The approach presented herein aims to reduce or eliminate the first-cycle irreversible capacity and enhance the thermal stability of the positive electrode, as presented and discussed in the following sections.

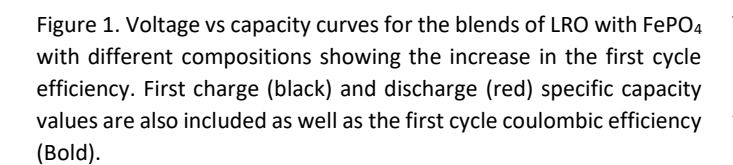
### Results and discussion

### Study of LRO and FePO<sub>4</sub> blended electrodes

Blends of LRO and FePO<sub>4</sub> were prepared in various weight fractions and electrochemically tested. Figure 1 shows the voltage vs. capacity profile for the first cycle of cells with LRO:FePO<sub>4</sub> blends, together with their corresponding capacity and coulombic efficiency values. For all compositions, the first oxidation reveals the high voltage plateau of LRO around 4.6V with its capacity gradually decreasing as the FePO<sub>4</sub> fraction in the blend increases. Interestingly, blends also showed a small plateau around 3.5 V, which likely indicates the existence of a minor amount of LFP. This feature does not appear to show a trend with fraction blend composition, suggesting possible lithium transfer between materials prior to cycling and/or microshorts during assembly. Upon reduction, all cells exhibit a similar voltage vs. capacity profile, starting with a sloping region that transitions to a flat plateau around 3.5V. As the fraction of FePO<sub>4</sub> in the blend increases, the plateau lengthens while the sloping region diminishes.

Journal Name ARTICLE





A similar trend is observed during reduction, where capacity decreases but remains relatively close to the expected values, as shown in Figure 2. Despite this, the coulombic efficiency improves significantly with blending, with the sample containing 33% FePO<sub>4</sub> achieving an efficiency of almost 100% (Figure 2). Further increasing FePO<sub>4</sub> content leads to coulombic efficiency values higher than 100%, with a maximum of 130% for 50% weight fraction. It is important to note that in full cells with graphite counter electrodes, the efficiency would not exceed 100%, the higher values achieved in the experiments presented herein are due to the use of lithium metal counter electrodes, which serve as an effectively unlimited lithium source. From the results discussed above it can be inferred that the optimal blend composition for practical applications is 33% FePO<sub>4</sub>, as it balances very high coulombic efficiency with higher capacity than blends with greater FePO<sub>4</sub> content.

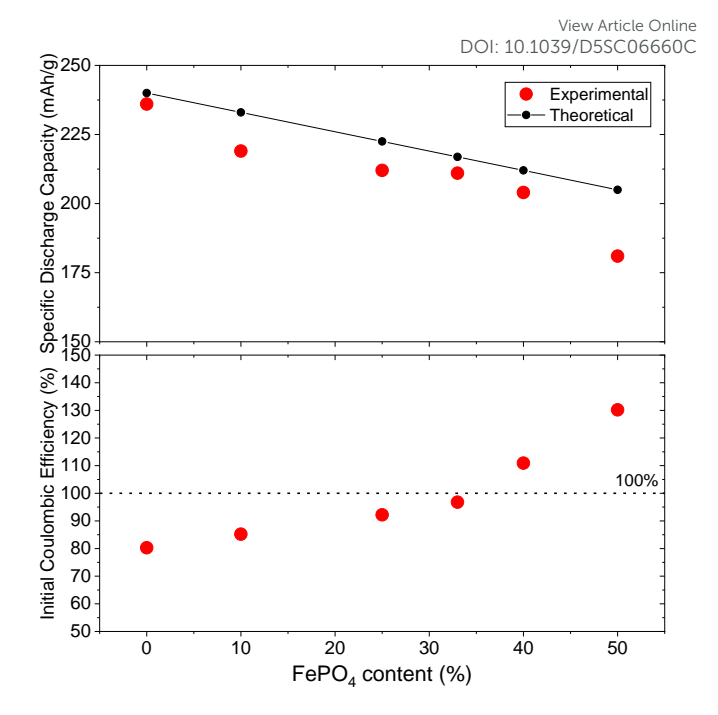


Figure 2. Experimentally measured and theoretical specific capacities (top), and 1st cycle coulombic efficiencies (bottom) of the studied electrodes. The black points and line show the theoretical capacity of the blends.

The evolution of capacity upon cycling was also studied for cells with 33% FePO<sub>4</sub>, 50% FePO<sub>4</sub> blends and pure LRO as positive electrode active materials. Figure 3 depicts the evolution of specific capacity for 100 cycles at 1C. The addition of FePO<sub>4</sub>, results in a significant improvement in capacity retention (after the 100th cycle values were found to be 86% for the pure LRO, 95% for the 33% FePO<sub>4</sub>:LRO blend and 98% for the 50% FePO<sub>4</sub>:LRO).

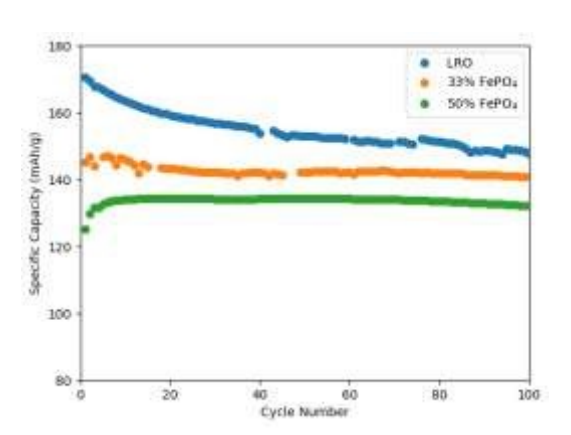


Figure 3. Evolution of specific capacity during 100 cycles at 1C rate between 2.0 and 4.6V, for pure LRO (blue), 33% FePO<sub>4</sub>:LRO (orange) and 50% FePO<sub>4</sub>:LRO (green).

This article is licensed under a Creative Commons Attribution-NonCommercial 3.0 Unported Licence

Open Access Article. Published on 17 2025. Downloaded on 2025/11/18 11:53:26.

**ARTICLE Journal Name** 

To evaluate the effect of blending on thermal stability, DSC was performed on oxidized electrodes consisting of pure LRO and a 33% FePO<sub>4</sub>:LRO blend (see experimental section in the SI). Additionally, two control experiments were conducted: one using a pure FePO<sub>4</sub> electrode, and another consisting only of the inactive components present in the electrode formulation (PVDF and carbon black).

Figure 4 shows the heat flow as a function of temperature for all electrodes. A sharp exothermic peak is observed for both LROcontaining electrodes, which is tentatively assigned to reactions involving the electrolyte and released O<sub>2</sub> from the electrode (13,32). The pure LRO sample shows its main process at 224.9°C with a released heat of 39.2 J/g. On the other hand, the 33% FePO<sub>4</sub> blend shows a peak temperature of 249.7 °C with a significantly reduced released heat (12.5 J/g). These results demonstrate that blending improves thermal stability by raising the decomposition onset temperature by ~25°C while reducing the released heat by more than two-thirds. In comparison, neither the pure FePO<sub>4</sub> nor the control experiment showed any exothermic processes within the tested range, confirming that the observed reactions originate from the LRO component.

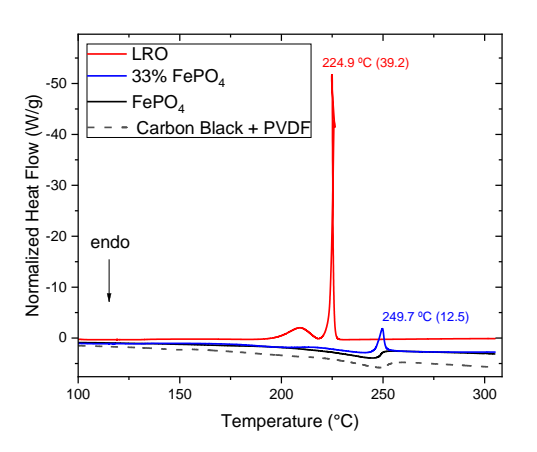


Figure 4. DSC curves of pure LRO (red line), pure FePO<sub>4</sub> (black line) and a LRO:FePO<sub>4</sub> blend containing 33% FePO<sub>4</sub> (blue line). A control experiment is also included (dashed black line) with electrodes containing no active material and only the PVDF binder and carbon black. Heating rate was 10 °C/min.

While these DSC results provide valuable insight into the thermal behaviour of the electrodes, it is worth highlighting that, to assertively assess the safety of the electrodes, more rigorous tests are needed using full cells and conditions closer to the ones that more closely replicate commercial batteries. Nonetheless, the observed increase in decomposition temperature and reduction in heat release suggest that blending LRO with FePO<sub>4</sub> may be a promising route toward safer electrode formulations. If these trends are maintained in more application-relevant conditions, blended 

### Influence of the additive's redox potential

Following the study of LRO blended with FePO<sub>4</sub> blend we investigated the effect of a second delithiated compound ( $\lambda$ -MnO<sub>2</sub>, the delithiated form of LMO (LiMn<sub>2</sub>O<sub>4</sub>) [30]) with a significantly higher lithiation potential. FePO<sub>4</sub> exhibits a redox potential around 3.5V vs Li<sup>+</sup>/Li while LRO starts delithiating at ca. 3.7V vs Li<sup>+</sup>/Li, which suggests minimal spontaneous lithium exchange between the two components prior to electrochemical cycling of the electrode. In contrast, λ-MnO<sub>2</sub> has a lithiation potential around 4.1V vs Li<sup>+</sup>/Li. The lithiation potentials of FePO<sub>4</sub> and λ-MnO<sub>2</sub> are shown in Figure 5 superimposed on the oxidation curve of LRO. At 4.1 V vs Li<sup>+</sup>/Li, LRO is expected to be partially oxidized and as such transfer lithium to  $\lambda$ -MnO<sub>2</sub> until the two potentials equilibrate. The amount of transferred lithium will depend on the relative quantities of the two materials and can significantly affect the electrode's sensitivity to humidity

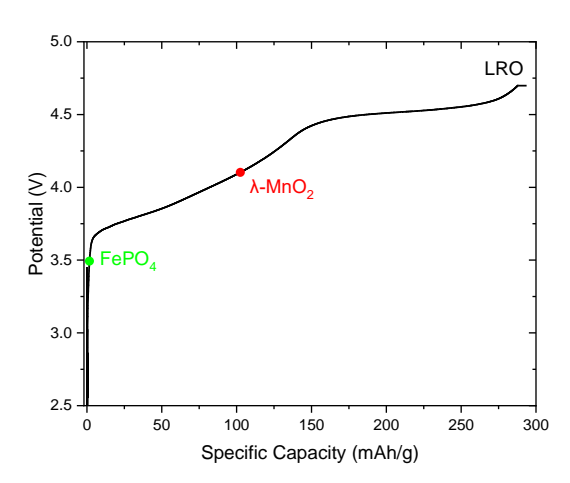


Figure 5. Potential vs. capacity profile corresponding to the delithiation of LRO, where the relative positions of the operation potentials corresponding to FePO<sub>4</sub> and λ-MnO<sub>2</sub> are depicted.

To test this hypothesis, two LRO:λ-MnO<sub>2</sub> blends of the same weight fraction were prepared, one in ambient conditions and one entirely in an argon filled glovebox with sub-ppm humidity. As seen in Figure 6, the electrode prepared in air exhibited a significantly lower reversible capacity (88mAh/g) while the one prepared in argon delivered 142mAh/g. The phenomenon is also reflected in the first cycle coulombic efficiency of the electrodes, which were 98% and 79% respectively. Since the increase in the coulombic efficiency is linked to lithium accessible vacancies, failure to increase it could indicate that those sites are already occupied by other species, possibly protons introduced after air exposure. These findings confirm that pre-oxidation of LRO, triggered by the high potential of This article is licensed under a Creative Commons Attribution-NonCommercial 3.0 Unported Licence

Open Access Article. Published on 17 2025. Downloaded on 2025/11/18 11:53:26.

Journal Name ARTICLE

 $\lambda$ -MnO<sub>2</sub>, can increase its vulnerability to environmental degradation. Preventing moisture exposure is therefore critical when using high-voltage additives to preserve lithium reinsertion capacity and maintain high efficiency.

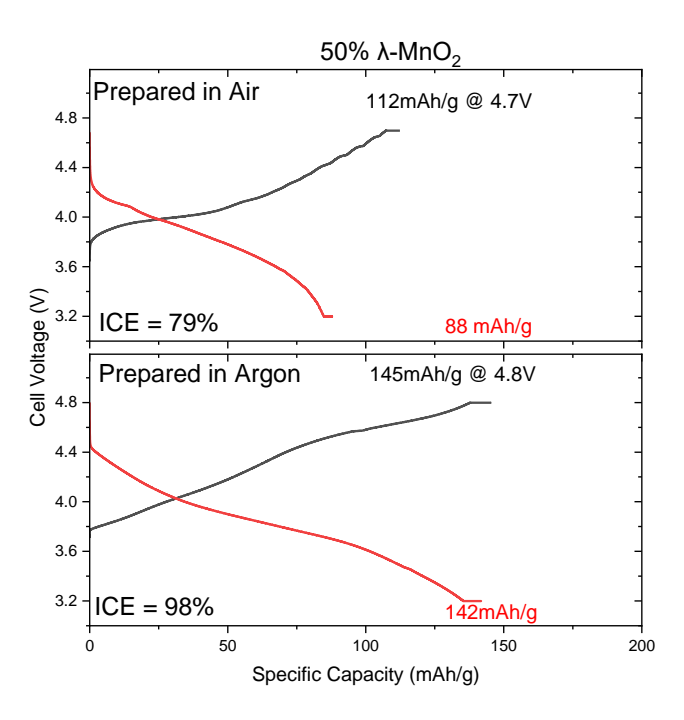


Figure 6 Voltage vs capacity profiles of 50% wt. LRO: $\lambda$ -MnO<sub>2</sub> blend prepared either in air (top) or inside an argon filled glovebox. Oxidation curves are depicted in black and reduction curves in red.

# Electrode dynamics in LRO:FePO<sub>4</sub> blends

In order to gain further insight into the electrode dynamics in LRO:FePO<sub>4</sub> blends, operando synchrotron X-ray diffraction was conducted. Electrodes with three different active material compositions were studied: pure FePO<sub>4</sub>, and the LRO blends with 33% FePO<sub>4</sub> and with 50% FePO<sub>4</sub>. Figure 7a shows the patterns corresponding to their first reduction at C/10 after oxidation to 4.8V at C/30. At 4.8V (yellow trace), the characteristic peaks of FePO<sub>4</sub> are visible with the most intense being the (200) at 4.8°, the (020) at 8.2° and the (121) at 9.7°, which provide a good guide to the eye for following the reaction. These peaks gradually decrease during reduction and, in accordance to the well-known phase transition reaction mechanism FePO<sub>4</sub>-LiFePO<sub>4</sub>, while new peaks corresponding to LiFePO<sub>4</sub> gain intensity as lithiation progresses: the (200) peak, this time around 4.6°, the (020) around 7.9° and the (311) around 9.4°. Peaks corresponding to LRO, exhibit their expected evolution, with the (003) appearing around 4.9° following a non monotonic behaviour, similarly to what is commonly observed in NMC systems. The (101) peak of LRO appears around 9.8° after full oxidation and shifts towards lower angles monotonically during reduction, as expected. Figure 7b shows the patterns of the 2nd oxidation and Figure 7c the corresponding capacity vs potential incurves. The evolution observed is the opposite of that seem during reduction, showing a good structural reversibility of the system. The 33% LRO:FePO4 blend exhibits a similar behaviour (Figure SI.2). It is clear after these experiments that FePO4 takes part in the cycling of such systems, capturing the excess lithium from the LRO. The system shows good reversibility making it feasible for use in next generation batteries.

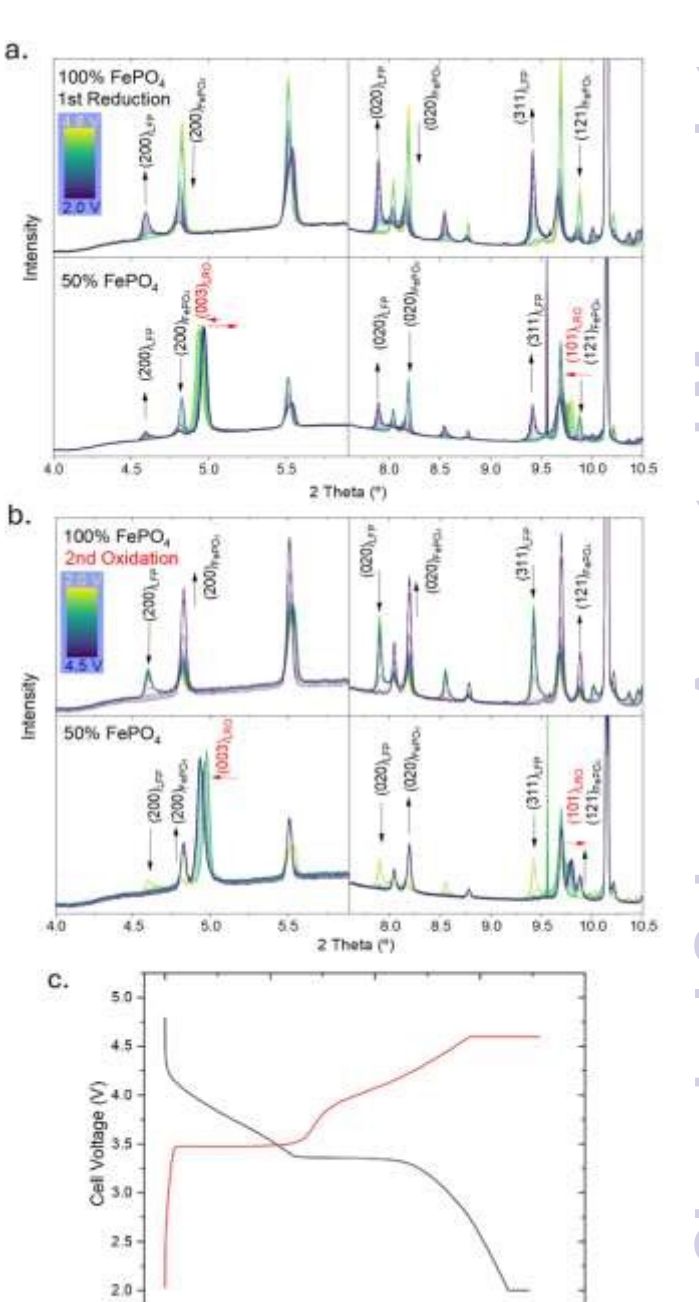


Figure 7: (a) Evolution of the diffraction patterns for pure FePO<sub>4</sub> and 50% FePO<sub>4</sub>:LRO throughout the first reduction, from yellow line (4.8V) to blue line (2V), (b) Same plot for the 2<sup>nd</sup> oxidation from yellow (2V) to blue line (4.5V). (c) Specific capacity vs potential curves of the depicted *operando* experiments.

100

Specific Capacity (mAh/g)

emical Science Accepted Manus

ARTICLE Journal Name

### **Conclusions**

A cobalt free, lithium rich layered oxide (LRO) with composition  $Li_{1.1s5}Ni_{0.3}Mn_{0.55}O_2$  was blended with chemically delithiated active materials, namely FePO $_4$  and  $\lambda\text{-MnO}_2$  to mitigate first cycle irreversibility and improve thermal stability and capacity retention. Blending with these lithium-acceptor compounds enabled reinsertion of lithium ions during the first charge, thereby reducing the irreversible capacity loss typically associated with the activation process in LRO. For the LRO - FePO<sub>4</sub> system, an optimal blend containing 33% FePO<sub>4</sub> was found to exhibit near zero first cycle irreversible capacity in half cells, better capacity retention, and enhanced thermal stability, with decomposition onset delayed by ~25 °C and a significant reduction in heat release. Operando synchrotron X-Ray diffraction confirmed the expected activity of FePO<sub>4</sub> validating its redox activity within the electrode and its ability to capture the excess lithium realeased by the LRO during activation. The LRO:λ-MnO<sub>2</sub> system appeared to be more complex due to the higher potential of  $\lambda\text{-MnO}_2$ , which induced partial LRO oxidation when mixing. This spontaneous lithium redistribution made the electrode more sensitive to moisture, significantly affecting performance unless handled in a dry atmosphere.

Overall, the results demonstrate that blending LRO with delithiated materials is an effective strategy not only to improve first-cycle efficiency but also to improve safety and mitigate capacity fading. These findings open a promising path for the rational design of highenergy, safer lithium-ion batteries. Future work should focus on scaling the approach to full-cell configurations and exploring long-term cycling stability under practical operating conditions.

### **Author contributions**

D. C.: Conceptualization, Investigation, Writing — original draft, Writing — review & editing. V.A.: Supervision, Writing — review & editing. P.E.C.: Supervision, Writing — review & editing. M. R. P.: Conceptualization, Supervision, Project administration, Funding acquisition, Writing — original draft, Writing — review & editing. M. C.C.: Conceptualization, Supervision, Project administration, Funding acquisition, Writing — original draft, Writing — review & editing.

### **Conflicts of interest**

There are no conflicts to declare.

### Data availability

Data for this article, including [description of data types] are available at DIGITAL.CSIC at [URL – format <a href="https://doi.org/DOI">https://doi.org/DOI</a>].

# **Acknowledgements**

This work has been done in the framework of the doctorate in Materials Science of the Universitat Autonomia de Barcelona and D.C. wants to acknowledge DESTINY MSCA PhD Programme, which has received funding from the European Union's Horizon 2020 research and innovation programme under Grant Agreement No 945357. ICMAB-CSIC members thank the Spanish Agencia Estatal de Investigación Severo Ochoa Programme for Centres of Excellence in R&D (CEX2023-001263-S) and funding through grant PID2023-146263NB-I00. MCC thanks Grant PID2022-1376260B-C33 funded by MCIN/AEI/10.13039/501100011033 and by "ERDF A way of making Europe" Authors are grateful for access to ALBA synchrotron for beamtime (proposals 2024028311 and 20250330058)

# References

- Whittingham MS. Lithium Batteries and Cathode Materials. Chem Rev. 2004 Oct 1;104(10):4271–302.
- Manthiram A. A reflection on lithium-ion battery cathode chemistry. Nat Commun [Internet]. 2020 Mar 25 [cited 2025 July 24];11(1). Available from: https://www.nature.com/articles/s41467-020-15355-0
- Casas-Cabanas M, Ponrouch A, Palacín MR. Blended Positive Electrodes for Li-Ion Batteries: From Empiricism to Rational Design. Israel Journal of Chemistry. 2021 Jan;61(1–2):26–37.
- Heubner C, Liebmann T, Lämmel C, Schneider M, Michaelis A. Internal dynamics of blended Li-insertion electrodes. Journal of Energy Storage. 2018 Dec;20:101–8.
- Chatzogiannakis D, Arcelus O, Ayerbe E, Ghorbanzade P, Ricci B, De Meatza I, et al. Key design considerations for blended electrodes in Li-ion batteries. Solid State Ionics. 2025 Oct;428:116942.
- 6. Smith AJ, Smith SR, Byrne T, Burns JC, Dahn JR. Synergies in Blended  $LiMn_2O_4$  and  $Li[Ni_{1/3}Mn_{1/3}Co_{1/3}]O_2$  Positive Electrodes. J Electrochem Soc. 2012;159(10):A1696–701.
- Tran HY, Täubert C, Fleischhammer M, Axmann P, Küppers L, Wohlfahrt-Mehrens M. LiMn2O4 Spinel/LiNi0.8Co0.15Al0.05O2 Blends as Cathode Materials for Lithium-Ion Batteries. J Electrochem Soc. 2011;158(5):A556.
- Chatzogiannakis D, Fehse M, Cabañero MA, Romano N, Black A, Saurel D, et al. Towards understanding the functional mechanism and synergistic effects of LiMn2O4 -LiNi0.5Mn0.3Co0.2O2 blended positive electrodes for Lithiumion batteries. Journal of Power Sources. 2024 Jan;591:233804.
- 9. Galushkin NE, Yazvinskaya NN, Galushkin DN. Causes and mechanism of thermal runaway in lithium-ion batteries, contradictions in the generally accepted mechanism. Journal of Energy Storage. 2024 May;86:111372.

This article is licensed under a Creative Commons Attribution-NonCommercial 3.0 Unported Licence

Access Article. Published on 17 2025. Downloaded on 2025/11/18 11:53:26.

**Journal Name ARTICLE** 

- 10. Dai Y, Panahi A. Thermal runaway process in lithium-ion batteries: A review. Next Energy. 2025 Jan;6:100186.
- 11. Doughty D, Roth EP. A General Discussion of Li Ion Battery Safety.
- 12. Shurtz RC, Hewson JC. Review—Materials Science Predictions of Thermal Runaway in Layered Metal-Oxide Cathodes: A Review of Thermodynamics. J Electrochem Soc. 2020 Jan 7;167(9):090543.
- 13. Hou J, Feng X, Wang L, Liu X, Ohma A, Lu L, et al. Unlocking the self-supported thermal runaway of high-energy lithium-ion batteries. Energy Storage Materials. 2021 Aug;39:395-402.
- 14. Yang H, Wu H, Ge M, Li L, Yuan Y, Yao Q, et al. Simultaneously Dual Modification of Ni-Rich Layered Oxide Cathode for High-Energy Lithium-Ion Batteries. Adv Funct Materials [Internet]. 2019 Mar [cited 2025 July 24];29(13). Available from: https://onlinelibrary.wiley.com/doi/10.1002/adfm.201808825
- 15. Schmitz RW, Murmann P, Schmitz R, Müller R, Krämer L, Kasnatscheew J, et al. Investigations on novel electrolytes, solvents and SEI additives for use in lithium-ion batteries: Systematic electrochemical characterization and detailed analysis by spectroscopic methods. Progress in Solid State Chemistry. 2014 Dec;42(4):65-84.
- 16. Sun G, Lai S, Kong X, Chen Z, Li K, Zhou R, et al. Synergistic Effect between LiNi $_{0.5}$ Co $_{0.2}$ Mn $_{0.3}$ O $_2$  and LiFe $_{0.15}$ Mn $_{0.85}$ PO $_4$ /C on Rate and Thermal Performance for Lithium Ion Batteries. ACS Appl Mater Interfaces. 2018 May 16;10(19):16458-66.
- 17. Rozier P, Tarascon JM. Review—Li-Rich Layered Oxide Cathodes for Next-Generation Li-Ion Batteries: Chances and Challenges. J Electrochem Soc. 2015;162(14):A2490-9.
- 18. Zuo W, Luo M, Liu X, Wu J, Liu H, Li J, et al. Li-rich cathodes for rechargeable Li-based batteries: reaction mechanisms and advanced characterization techniques. Energy Environ Sci. 2020;13(12):4450-97.
- 19. Assat G, Tarascon JM. Fundamental understanding and practical challenges of anionic redox activity in Li-ion batteries. Nat Energy. 2018 Apr 9;3(5):373-86.
- 20. Jang HY, Eum D, Cho J, Lim J, Lee Y, Song JH, et al. Structurally robust lithium-rich layered oxides for high-energy and longlasting cathodes. Nat Commun [Internet]. 2024 Feb 12 [cited 2025 July 24];15(1). Available from: https://www.nature.com/articles/s41467-024-45490-x
- 21. Zhang M, Kitchaev DA, Lebens-Higgins Z, Vinckeviciute J, Zuba M, Reeves PJ, et al. Pushing the limit of 3d transition metalbased layered oxides that use both cation and anion redox for energy storage. Nature Reviews Materials. 2022 July 1;7(7):522-40.
- 22. Lin T, Seaby T, Hu Y, Ding S, Liu Y, Luo B, et al. Understanding and Control of Activation Process of Lithium-Rich Cathode Materials. Electrochem Energy Rev. 2022 Dec;5(S2):27.

- 23. Deng Z, Liu Y, Wang L, Fu N, Li Y, Luo Y, et al. Challenges of Online thermal stability of high-energy layered oxide wathouse 0066600 materials for lithium-ion batteries: A review. Materials Today. 2023 Oct;69:236-61.
- 24. Pan H, Jiao S, Xue Z, Zhang J, Xu X, Gan L, et al. The Roles of Ni and Mn in the Thermal Stability of Lithium-Rich Manganese-Rich Oxide Cathode. Advanced Energy Materials [Internet]. 2023 Apr [cited 2025 July 24];13(15). Available from: https://onlinelibrary.wiley.com/doi/10.1002/aenm.202203989
- 25. Gao J, Manthiram A. Eliminating the irreversible capacity loss of high capacity layered Li[Li0.2Mn0.54Ni0.13Co0.13]O2 cathode by blending with other lithium insertion hosts. Journal of Power Sources. 2009 June;191(2):644-7.
- Gao J, Kim J, Manthiram A. High capacity Li[Li0.2Mn0.54Ni0.13Co0.13]O2-V2O5 composite cathodes with low irreversible capacity loss for lithium ion batteries. Electrochemistry Communications. 2009 Jan;11(1):84-6.
- 27. Zhou L, Yin Z, Ding Z, Li X, Wang Z, Wang Y. Bulk and surface reconstructed Li-rich Mn-based cathode material for lithium ion batteries with eliminating irreversible capacity loss. Journal of Electroanalytical Chemistry. 2018 Nov;829:7-15.
- 28. Hu X, Guo H, Wang J, Wang Z, Li X, Hu Q, et al. Structural and electrochemical characterization of NH4F-pretreated lithiumrich layered Li[Li0.2Ni0.13Co0.13Mn0.54]O2 cathodes for lithium-ion batteries. Ceramics International. 2018 Aug;44(12):14370-6.
- 29. Zheng J, Deng S, Shi Z, Xu H, Xu H, Deng Y, et al. The effects of persulfate treatment on the electrochemical properties of Li[Li0.2Mn0.54Ni0.13Co0.13]O2 cathode material. Journal of Power Sources. 2013 Jan;221:108-13.
- 30. Lu Z, MacNeil DD, Dahn JR. Layered Cathode Materials Li [ Nix Li (1/3-2x/3) Mn (2/3-x/3) O 2 for Lithium-lon Batteries. Electrochemical and Solid-State Letters. 2001 Sept 13;4(11):A191.
- 31. Johnson CS, Kim JS, Lefief C, Li N, Vaughey JT, Thackeray MM. The significance of the Li2MnO3 component in 'composite' xLi2MnO3·(1-x)LiMn0.5Ni0.5O2 electrodes. Electrochemistry Communications. 2004 Oct;6(10):1085-91.
- 32. Zhang Z, Fouchard D, Rea JR. Differential scanning calorimetry material studies: implications for the safety of lithium-ion
- 33. Xu P, Guo X, Jiao B, Chen J, Zhang M, Liu H, et al. Protonexchange induced reactivity in layered oxides for lithium-ion batteries. Nat Commun. 2024 Nov 13;15(1):9842.

# **Data availability**

Data for this article, including [description of data types] are available at DIGITAL.CSIC at [URL – format <a href="https://doi.org/DOI">https://doi.org/DOI</a>].